An overview of multicarrier predistortion techniques and associated throughput gain for an actual hardware implementation

Dieter Duyck* , Alberto Mengali and M.R. Bhavani Shankar† , Konstantinos Liolis ‡,
Cedric Le Guern, Boris Tiomela Jou § , S. Cioni ¶

Efficiency gain is a relevant metric of communication technology, as it directly translates to the same improvement in operational expenditures, while sometimes also allowing capital expenditure gains. The latest multicarrier predistortion techniques for satellite communications yield significant throughput gains. However, there has been no publication yet of such a technique, achieving large gains for realistic linearized transponders, that is also sufficiently low complex in hardware resources allowing implementation on actual modulators. We have implemented improvements of existing techniques allowing such implementation, validated by means of simulations. This paper provides an overview of the state of the art of (multicarrier) predistortion as well as simulation results of the best selected techniques as well as our improvement, over multiple transponder types. For out improvement of iterative cancellation predistortion technique, throughput gains in the order of 10% were found over challenging linearized transponders by increasing the symbol rate while maintaining the occupied bandwidth. It is our expectation that those gains will be demonstrated in the near future through an actual hardware implementation.

I. Introduction

I.A. Background

Due to the large distances to be bridged in satellite communications, power is a scarce resource. Therefore, the on-board amplifier, typically a travelling wave tube amplifier (TWTA) is driven close to saturation, making the aggregate satellite channel non-linear (NL).

Predistortion improves the error rate performance for transmission over NL channels. Due to the presence of the pulse-shaping filter in the modulator and the matched filter in the receiver, the symbol-level channel between the transmitted and received symbols is a non-linear channel with memory. This non-linear symbol-level channel with memory mainly impairs the received baseband symbol sequence after the matched filter in the following two ways [9]:

- in a scatter plot, each constellation point becomes a cluster, caused by intersymbol interference (ISI); for multi-carrier transmission, the ISI caused by the non-linear channel with memory can be divided

*Technical Labs, Newtec
†Interdisciplinary centre for Security, Reliability and Trust (SnT), University of Luxembourg
‡SES S.A.
§Airbus
¶European Space Agency, TEC-EST Section

in two categories: self-interference, for ISI with symbols sent over the same carrier, and inter-carrier interference, for ISI with symbols sent over other carriers (sometimes referred to as adjacent channel interference (ACI) [3]);

- constellation warping - causing the mass points of the clusters to be no longer on the received constellation grid. The first effect (forming of the clusters) is considered to be the most harmful to the error rate performance [9]. Serious warping can be very harmful as well, but it is easier to cancel than ISI.

With the next generation of satellites, especially high throughput satellites, it is more common to have significantly larger bandwidths per transponder. This leads to a more frequent adoption of multicarrier transmission, also in the forward link from hub to terminal. Typically, these transponders are linearized, meaning that they have a limited small signal gain, e.g. 3 dB, and a limited phase rotation. As efficiency is a key differentiator in the forward link, *multicarrier predistortion for linearized transponders* becomes a very important requirement for advanced modulators.

1. Contribution of this paper

In this paper we present a brief overview of selected categories of predistortion available in the literature. We subsequently focus on the most promising multicarrier predistortion techniques that are sufficiently low complex allowing implementation in actual modulators.We compare those techniques in terms of total degradation, for a fixed scenario[a], obtained by means of simulation over typical transponder models. We also present results for an improvement of the state of the art that we made in order to achieve the best performance gains while still allowing an actual hardware implementation. Finally, we compute the average throughput gain within a given occupied bandwidth achieved by our improved technique.

II. Literature overview

We focus on *digital* predistortion (DPD) algorithms which is easier to implement, more adaptive, and which achieves better performance than analog predistortion. A basic DPD technique is referred to as static symbol-level DPD [11] or static distortion compensation [10], which statically changes the transmit constellation in order to combat constellation warping. The channel-dependent transmit constellation modification occurs off-line and is valid on a long term (aging and temperature sensitivity of the transponder may modify the transponder gain, compensated by the automatic level control (ALC), but do not modify the AM/AM and AM/PM characteristics [8]). A more advanced predistortion technique is referred to as dynamic symbol-level DPD [11] or dynamic data DPD [8]. It was first proposed by [10]. In this technique, new transmit symbols are chosen, based on the *neighbouring*[b] symbols (it thus defines a new multidimensional constellation grid). It outperforms static symbol-level DPD because it also reduces the cluster forming in the scatter plot at the receiver.

In a conventional implementation, dynamic symbol-level DPD is look-up table (LUT) based and therefore requires a lot of memory (to store the multidimensional constellation) and off-line computations (to compute the multidimensional constellation). It therefore consumes too much memory for single carrier transmission and constellations of 64 or more points. Even for lower constellation sizes, the assumed channel memory size is still much too low as for example a true memory size of 32 with a 32-APSK constellation (which would require a 32^{32} size LUT) requires too much memory. Furthermore, for multicarrier transmission, this

[a]The fixed scenario consists of a fixed modcod (32APSK56), 20% roll-off, and a fixed symbol rate per carrier, without overlapping the carriers in the frequency domain.

[b]Neighbouring symbols is referred to in time, but also in frequency (neighbouring carriers) for multicarrier transmission.

memory is taken to the power of the number of carriers as well; the multi-dimensional constellation size not only grows with the memory of the channel, but also with the number of neighbouring carriers. Fortunately, dynamic symbol-level DPD can be equivalently implemented without resorting to multidimensional maps. In fact, polynomial based symbol-level DPD, discussed in Sec. IV, is shown to achieve good performance results even when compared to map based solutions [15, 14].

Besides considering the symbol domain (before the pulse-shaping filter (PSF)), DPD can also be performed in the signal or sample domain, which mainly acts after the PSF of the transmitter. In contrast to a conventional implementation of symbol-level DPD, the computational complexity does not increase with the number of points in the constellations or with the number of carriers, making it attractive for implementation of multicarrier DPD. Assuming linear distortions are compensated for, the memory of the non-linear sample-level channel is zero, allowing powerful DPD with low implementation complexity. On the other hand, sample-level DPD technique intends to compensate distortions realized in the sample-level channel. However, distortions occurring outside of the channel (e.g. due to non-orthogonal signaling, such as carriers partly overlapping in frequency) cannot be tackled. It also has more difficulties to tackle distortion from linearized transponders, which mainly come from the TWTA behaviour on and beyond saturation.

Finally, a new class of iterative or successive DPD techniques [1, 2, 4] is discussed. This new class combines the advantages of the previous techniques, i.e., it acts on the symbol-level, which allows it to tackle distortions from linearized transponders and from non-orthogonal signaling, while its complexity does not grow with the constellation size and is only linear (and not exponential) in the number of carriers. We also present for the first time results for an an improvement over this technique, first introduced in [7, 20].

Below, after presenting the channel model (Sec. III), we elaborate in Sec. IV on polynomial based symbol-level DPD algorithm, followed by signal DPD and iterative DPD techniques.

III. System Model and metric used to compare most promising techniques

For conciseness and clarity, we limit the system model to a specific example. Consider a scenario where 4 carriers are uplinked to the same transponder. Denote the symbols of carrier c before the pulse-shape filter by $a_c[k]$ where k is the symbol time index. After the PSF, we get the samples $s_c[l]$, where l is the sample time index, where each sample $s_c[l]$ is a linear combination of a number of symbols. The multicarrier signal $s[l]$ is the result of mixing the samples of each carrier with their corresponding baseband carrier frequency and adding the mixed samples of all carriers.

The satellite channel between the modulator and receiver can be simplified as the concatenation of an input multiplexing (IMUX) filter, a non-linear TWTA, and an output multiplexing (OMUX) filter. DPD only improves downlink noise limited channels (e.g. forward links with hubs with big earth station antennas and smaller terminal antennas). Thus, often the uplink noise is ignored, as is the case here (but sensitivity tests to limited uplink noise have been performed to verify operation usability). Making abstraction of input and output filter stages of the TWTA (which is justified when the occupied bandwidth of the signal is within the bandwidth of the filters preceding and following the amplifier), we can model the non-linear channel before additive white Gaussian noise (AWGN) addition at the earth receiver as a memoryless baseband equivalent function $\mathcal{F}_{\mathrm{NoMem}}(.)$. It is customary to model the amplitude and phase of $\mathcal{F}_{\mathrm{NoMem}}(.)$, referred to as AM/AM and AM/PM characteristics, respectively, with two different functions $\mathcal{A}$ and $\mathcal{Z}$, yielding

$$\mathcal{F}_{\mathrm{NoMem}}(x) = \mathcal{A}[A_{in}] \times \exp\left(i\left(\mathcal{Z}\left[A_{in}\right] + \angle x\right)\right),$$

where we denote the input magnitude of the channel $A_{in} = |x|$ and the output magnitude of the channel

$A_{out} = \mathcal{A}[|A_{in}|]$, and where $\angle x$ refers to the phase of x. The saturation point corresponds to the maximum of A_{out}. There exist multiple TWTA models for $\mathcal{F}_{\text{NoMem}}(.)$, such as the modified Saleh model [12].

Please note that typically the output magnitude of the modified Saleh model decreases after saturation, so that there does not exist a function $\mathcal{A}^{\text{inv}}$, such that $\mathcal{A}\left[\mathcal{A}^{\text{inv}}[\mathcal{A}_{in}]\right], \ \forall A_{in}$. Therefore, often the clipped AM/AM function is considered,

$$\begin{aligned} \mathcal{A}_{\text{clip}}[A_{in}] &= \mathcal{A}[A_{in}], \ \forall A_{in} \leq 1 \\ \mathcal{A}_{\text{clip}}[A_{in}] &= 1, \ \forall A_{in} > 1, \end{aligned}$$

as this function does have an inverse.

In this paper, we consider three functions $\mathcal{F}^1_{\text{NoMem}}(.)$, $\mathcal{F}^2_{\text{NoMem}}(.)$ and $\mathcal{F}^3_{\text{NoMem}}(.)$, shown in Fig. 1, referred to as tube 1, tube 2, and tube 3. Tubes 2 and 3 have a small signal gain of 3 dB, and almost no phase rotation. Tube 2 has a significant fall-back beyond saturation. Tube 1 is a typical non-linear tube with a small signal gain around 7 dB and a signifant phase rotation around and beyond saturation.

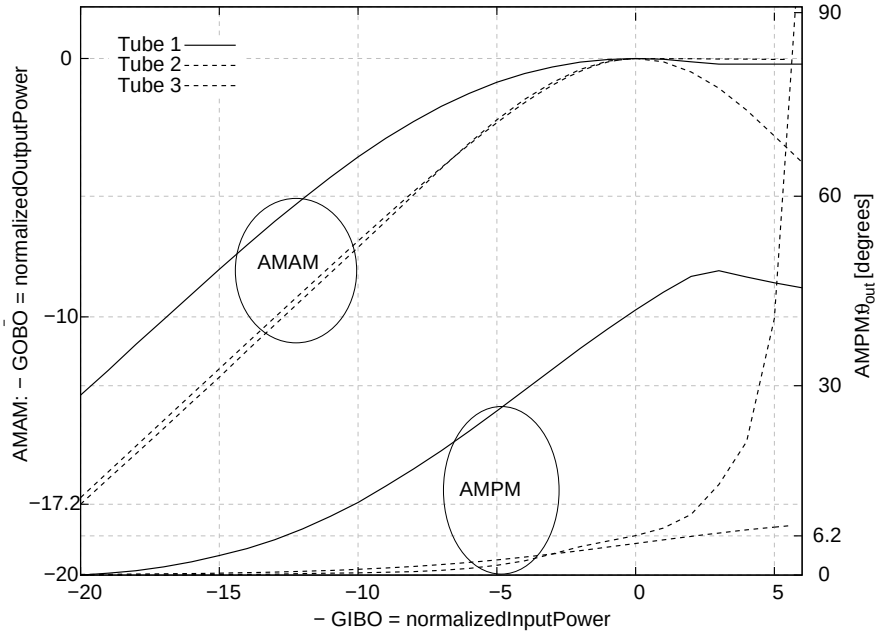

Figure 1. The considered transponders (AM/AM and AM/PM characteristic) for the simulations reported in this paper.

The relevant simulation parameters of the transmitter and receiver are provided in Table 1

Typically, the DPD *gain* is expressed as *total degradation gain* achieved over a given non-linear channel [9, 3, 5, 6]. This paper reports results obtained in [20], in which a first assessment and decision criterium for the available predistortion techniques was based on TD gain for Tubes 1 and 2. The selected technique based on TD gain will then be further investigated in terms of throughput [6], for all three tubes.

IV. Presentation and comparison of most promising predistortion techniques

DPD can be applied either on the baseband *symbols* (before the PSF) and/or the waveform *samples* (after the PSF). The former allows for design and implementation of the DPD at a rate equal to the symbol rate, thereby reducing power consumption for small symbol rates. However, they are disdvantaged by the fact that they have access only to the bandwidth occupied by the pulse shaping filter. For example, only

Table 1. Scenario

Parameter	Value
Transponder BW	36 MHz
Pulse Shaping Filter	SRRC
SRRC Filter Taps	24 (symbol level), 408 (sample level)
Roll-off	20%
Number of carriers	4
Carrier Spacing	1 + Roll-off
MODCOD	32-APSK 5/6
Baudrate	7.5 Mbaud
BCH	Yes

manipulating the symbols does not generate spectral regrowth and thus only provides for *in-band* distortion compensation [16].

On the other hand, the non-linear channel acts on the modulated waveform (after the PSF), so that it is natural to predistort the signal after the PSF as well, referred to as sample-level or signal DPD. Indeed, due to the presence of the PSF in the modulator and the matched filter in the receiver, the symbol-level channel between the transmitted and received symbols is a non-linear channel with memory, which is hard to model. On the other hand, assuming IMUX and OMUX filters are perfect passband filters[c], the sample-level channel between the transmitted samples (after the PSF) and the received samples (before the matched filter) is a memoryless channel [9]. Thus sample-level DPD is fairly straightforward and low complex. Furthermore, by definition, signal predistortion is the same for single carrier as for multicarrier systems as in both cases, there is only one waveform to be processed. The only difference can lie in slightly different parameters and different performance results.

In this section, we discuss the most promising predistortion techniques based on the literature on symbol-level DPD (Sec. IV.A), sample-level DPD (Sec. IV.B), and a combination of both (Sec. IV.C).

IV.A. Polynomial based symbol-level predistortion

Fig. 2 presents the simplified block diagram of a multicarrier symbol-level DPD; here $u_k(\cdot)$ and $x_k(\cdot)$ refer to the symbol stream on the kth carrier before and after the symbol-level DPD, p_k is the pulse shaping filter, f_k is the frequency upconversion, and MASK is the uplink filter or low pass filter that limits the uplink out-of-band emissions according to regulations. The multicarrier symbol-level DPD acts jointly on all the streams to effect predistortion.

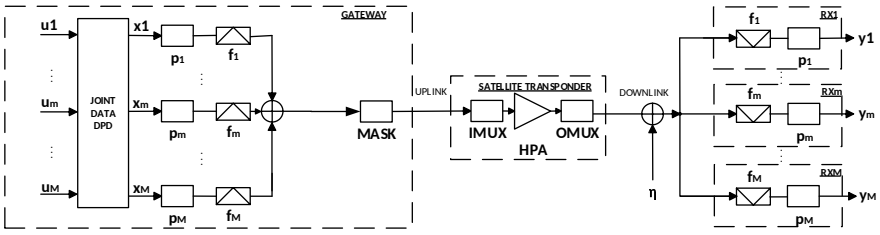

Figure 2. Simplified block diagram of polynomial based symbol-level DPD.

Building on the multicarrier data model provided in [3], several symbol-level DPD techniques (sometimes

[c]This is not the case, but it is an interesting first approximation.

referred to as joint data predistortion in the context of multicarrier transmission) have been considered in the literature [14, 15]. Rather than implementing large multi-dimensional maps, these techniques are based on polynomial functions that jointly process the data symbols from all carriers. Without going into detail, a multicarrier memory polynomial function can be defined as,

$$x_m(n) = \sum_{m_i} \sum_{k} h_{m,m_i}(k) u_{m_i}(n-k) + \sum_{m_i,m_j,m_z} \sum_{k_i,k_j,k_z} h_{m,m_i,m_j,m_z}(k_i,k_j,k_z) u_{m_i}(n-k_i) u_{m_j}(n-k_j) u^*_{m_z}(n-k_z) \tag{1}$$

where $u_m(n)$ is the data symbol relative to the m th carrier at the n th time instant, $h_\cdot(\cdot)$ are the coefficiencts of the Volterra[d] expansion of the channel inverse and $x_m(n)$ is the resulting predistorted symbol. The terms k_* refer to memory while m_* refer to carrier index. The model above assumes that the order of the non-linearity is three (higher orders are negligible). The identification of the coefficients relies on training and is carried out using the standard *indirect approach* [14, 15]. The indirect approach is based on the fact that in the absence of noise, the precompensation (predistortion) is equivalent to the post compensation (equalization) when the channel function is invertible. Further improvement in performance can be obtained by improved estimation of the predistorter coefficients: optimization methods for estimating the predistorter coefficients are discussed in [16] for multicarrier satellite systems. In the current set up, a simplified training procedure based on the indirect paradigm using a low noise receiver is considered. In particular, since the receiver noise is neglected, gains of direct DPD over the indirect are negligible.

The disadvantage of symbol-level DPD is that the complexity of implementing 1 is too high for non-linear symbol-level channels with a large memory. Approximations in this modeling can lead to large performance degradations.

IV.B. Sample-level predistortion

In [14, 3], the first approximation on IMUX and OMUX filters being ideal passband filters is lifted and the sample-level channel is considered as a non-linear channel with memory, modeled using the Volterra series. In general, Volterra-based DPD is generally applicable to any non-linear channel with memory because its representation is complete.

In block-structured DPD, the non-linearity on the one hand and the memory on the other hand are compensated for separately; the memory is compensated for with a linear filter and the non-linearity is compensated for with a memoryless non-linear function implemented with a LUT. Block-structured sample-level DPD is indeed a special case of Volterra-based sample-level DPD. However, block-structured sample-level DPD leaves the paradigm of modeling the non-linear channel with memeory and starts from the actual satellite non-linear channel which brings immediate complexity reduction gains[e].

Provided enough training is performed, Volterra based sample-level DPD outperforms block-structured sample-level DPD [17]. However, practically as good performance can be achieved by tackling IMUX distortions with a linear filter and the TWTA with a memoryless non-linear function [13]. Thanks to the low complexity, high performance for non-linear channels with large ssg's (small signal gains), and easy calibration, block-structured DPD is very interesting for commercial applications.

The main drawback of sample-level DPD is that the inverse AMAM function does not exist, as the AMAM function falls back beyond saturation. Therefore, the above mentioned LUT typically implements the inverse

[d] A Volterra series representation is a complete representation for non-linear systems in general in the Stone-Weierstrass theorem sense [18, 19], and therefore popular from an academic point of view.

[e] This new paradigm also facilitates calibration where the parameters of an unknown actual channel are looked for. First taking sufficient backoff, the parameters of the IMUX and OMUX can be found. After conseqeuntly applying the inverse linear filter, the parameters of the remaining non-linear memoryless channel can be found.

of the simplified AMAM function $\mathcal{A}_{\text{clip}}[A_{in}]$. For application with a drive-level close to saturation, as well as for linearized transponders (where the main non-linearity is the saturation and the AMAM function beyond saturation), sample-level DPD falls short.

Finally, the symbol-level channel can have additional distortions when using non-orthogonal signaling. As sample-level DPD is located inside, rather than in front of this symbol-level channel, it is not intended to compensate for these additional distortions, which brings it in disadvantage with respect to symbol-level DPD.

The disadvantages mentioned above for symbol-level DPD (difficulty to model the non-linear symbol-level channel with memory) amd sample-level DPD (performance degradation for linearized transponders and non-orthogonal signaling) bring us to the last technique discussed in the following section.

IV.C. Iterative or successive predistortion

Initially, this type of predistortion was introduced in [1], followed by [2]. It is an iterative algorithm, where each successive interference cancellation (SIC) iteration applies a symbol-level transmission link *model* (i.e a transmit filter, TWTA and receive filter) to the symbols at its input. It then computes the difference between the received symbols and a target constellation. In order to compensate for this difference, a new set of transmit symbols are obtained by adding this difference to the symbols it received at its input, and these corrected transmit symbols are then handed to the next SIC iteration. In [4], 20 iterations were performed to obtain the reported results. The main reason why this technique outperforms previous symbol-level DPD techniques is because there is no need to analytically model the non-linear channel with memory. The technique basically measures the input-output relation of this channel for a given input, implementing a very large memory which would not be feasible for previous symbol-level DPD techniques. That way, less modeling approximations are made.

Because of the high number of iterations in [4], this technique appeared unfeasible until today. Fortunately, an improvement was proposed in [7, 20] which allowed to significantly reduce the number of iterations without sacrificing performance. The main aspect lies in combining symbol-level and sample-level DPD to fastly reach convergence. We refer to [4, 7, 20] for further details. However, we do present below simulation results for our improvement.

IV.D. Simulation results for tubes 1 and 2

Table 2 provides the TD gains achieved for the techniques above for tubes 1 and 2. For successive DPD, 3 SIC iterations were performed.

Table 2. The TD gains achieved for the presented techniques for tubes 1 and 2.

Technique	Tube	TD gain [dB]
polynomial-based symbol-level DPD	1	1.34
sample-level DPD	1	2.83
Successive DPD	1	4.34
polynomial-based symbol-level DPD	2	0.26
sample-level DPD	2	0.31
Successive DPD	2	1.16

We also simulated the gain of [4] over tube 2, which featured a TD gain of 0.5 dB, even with 9 SIC iterations. Due to the fallback beyond saturation, measures have to be taken [7, 20] to guarantee convergence.

The same measures lead to a faster convergence on other tubes. For example, for tube 1, the TD gain of [7, 20] is 4.34 dB with 3 SIC iterations, while [4] needs 20 SIC iterations to reach a comparable gain of 4.7 dB.

Based on those results, successive DPD [7, 20] was selected for implementation and further investigation, see Sec. V.

V. Throughput gain of selected iterative predistortion

Successive DPD is perfectly fit to not only compensate for channel distortions, but also for distortions due to non-orthogonal signaling (such as Faster than Nyquist or frequency overlapping of carriers). Therefore, the true metric is to maximize the throughput gain within a given occupied bandwidth [6]. Here, the occupied bandwidth is 36 MHz. This limited occupied bandwidth allowed us to go to 5 SIC iterations.

On the other hand, we only looked at the results of the VHDL implementation of the successive DPD. To allow a VHDL implementation, we had to apply some slight simplifications, such as a limited oversampling rate and time-synchronization of each of the carriers, which lead to a small degradation w.r.t. to the simulation results reported in Sec. IV.D.

More specifically, the TD gain of successive DPD with 5 SIC iterations with hardware limitations for tube 2 reduced to 0.82 dB and 1.5 dB for tube 3. It can be concluded that the fallback beyond saturation plays a big role in the TD gain achieved, even for the improved successive DPD technique from [7, 20]. With orthogonal signaling, the average throughput gain averaged over SNRs uniformly distributed between 19 and 24 dB is 6.2%. However, if we allow to overlap the carriers in frequency (by increasing the symbol rate but changing the carrier frequencies such that the occupied bandwidth remains the same), the gain of successive DPD w.r.t. the baseline scenario is 8.6% (with carrier overlapping in the baseline scenario) and 9.6% (without carrier overlapping in the baseline scenario). This is computed by taking the ratio of the areas below the staircase curves for each of the scenarios for an academic ACM example, see Fig. 3 (see [6] for more information).

VI. Conclusion

We provide a qualitive overview of multicarrier predistortion techniques based on literature results for three transponder models. We took into account constraints allowing an actual hardware implementation. We conclude that successive interference cancellation (SIC) techniques manipulating the transmit signal both on the symbol-level (before the pulse-shaping filter) as on the sample-level (after the pulse-shaping filter) significantly outperform the other techniques. Furthermore, its complexity does not scale with the constellation size, and scales only linearly with the number of carriers. Finally, SIC techniques are perfectly fit to non-orthogonal signaling which allow to increase the spectral efficiency further. The average throughput gain over a linearized transponder with significant fallback beyond saturation approaches 10% which is exceptional and of real value to satellite operators and service providers. This technique is now part of a real hardware demonstrator, the presentation of which is outside the scope and timing of this paper. The laboratory and field validation results of the technology under consideration correspond to future work, which will be presented in another paper.

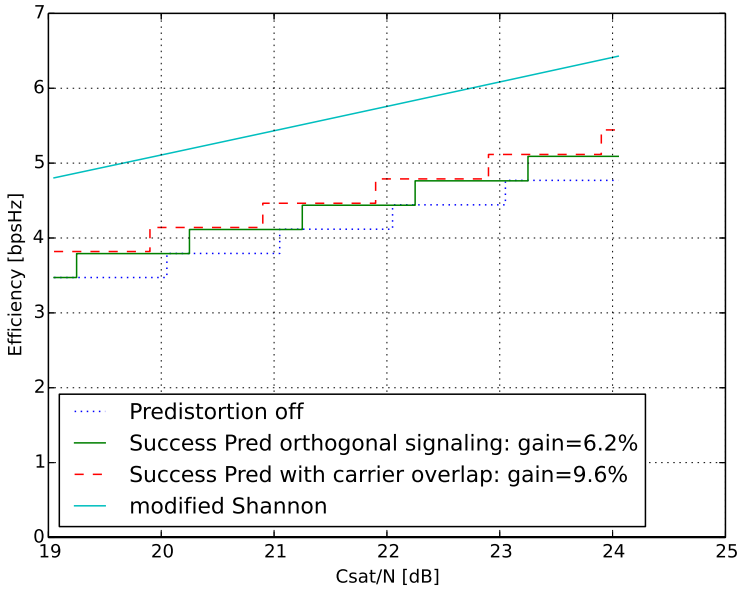

Figure 3. The ACM performances with successive predistortion and with (dashed) and without (lowest full line) orthogonal signaling over the considered channel, compared to the ACM performances without predistortion and orthogonal signaling (dotted) and the modified Shannon bound.

Acknowledgments

This research was developed within the framework of ESA-funded project "Prototyping and Testing of efficient multicarrier transmission for broadband satellite communications", Ctr. nr 4000112692. We also thank other contributors in this project which are not part of the author list, such as Joel Grotz, Patricia Inigo, Olivier De Dedeken, Roberto Piazza, Oriol Vidal, and Alastair Isaacs.

References

[1]B.H. Beech and D.G. Edwards, "Method and apparatus for reducing distortion of digital data," patent EP1129556 B1.

[2]B.H. Beech, D.G. Edwards, and R. Perinpanayagam, "Method and apparatus for reducing distortion of digital data," patent EP1371202 B1.

[3]B. F. Beidas, "Intermodulation distortion in multicarrier satellite systems: Analysis and turbo Volterra equalization," IEEE Trans. Commun., vol. 59, no. 6, pp. 1580 1590, June 2011.

[4]B.F. Beidas, R.I. Seshadri and N. Becker, "Multicarrier successive predistortion for nonlinear satellite systems," IEEE Trans. on Comm., vol. 63, no. 4, pp. 1373-1382, April 2015.

[5]E. Casini, R. De Gaudenzi, A. Ginesi, "DVB-S2 modem algorithms design and performance over typical satellite channels," in Int. J. Satell. Commun. Network., vol. 22, pages 281318, 2004m doi:10.1002/sat.791.

[6]D. Duyck, A. Mengali, et al., "The correct gain metric to assess predistortion techniques," AIAA Intern. Comm. Sat. Systems Conf. (ICSSC), Oct. 2017.

[7]D. Duyck and O. De Deken, "Transmitter,", Patent publication PCT/EP2016/082008.

[8]R. De Gaudenzi, A. Guillen I Fabregas, and A. Martinez, "Performance Analysis of Turbo-Coded APSK Modulations over Nonlinear Satellite Channels," IEEE Trans. on Wireless Comm., vol. 5, no. 9, pp. 2396- 2407, Sept. 2006.

[9]G. Karam and H. Sari, "A Data Predistortion Technique with Memory for QAM Radio Systems," IEEE Tr. On Comm., vol. 39, no. 2, pp. 336-344, Feb. 1991.

[10]G. Karam and H. Sari, "Data predistortion techniques using intersymbol interpolation," IEEE Trans. On Comm., vol. 38, no. 10, pp. 1716 1723, Oct. 1990.

[11]F. Kayhan and G. Montorsi, "Constellation Design for Transmission over Nonlinear Satellite Channels," submitted to Trans. On Inf. Theory, Oct. 2012.

[12]G. Maral and M. Bousquet, "Satellite Communications Systems, 5th edition," Wiley, 2009.

[13]M. Allegue-Martnez, N. Kelly and A. Zhu, "Digital linear pre-compensation technique to enhance predistortion performance in multicarrier DVB-S2 satellite communication systems," Electr. Letters, June 2014, vol. 50, no. 13, pp. 957-959.

[14]R. Piazza, B. Shankar, E. Zenteno, D. Rnnow, J. Grotz, F. Zimmer, M. Grasslin, F. Heckmann, and S. Cioni, "Multicarrier Digital Pre-distortion/ Equalization Techniques for Non-linear Satellite Channels," Proc. Of 30th AIAA International Communications Satellite Systems Conference (ICSSC), Ottawa (Canada), 24-27 Sep. 2012.

[15]R. Piazza, B. Shankar, and B. Ottersten, "Non-parametric data predistortion for non-linear channels with memory," in IEEE International Conference on Acoustics, Speech, and Signal Processing (ICASSP), 2013. [Online]. Available: http://orbilu.uni.lu/handle/10993/4862

[16]R. Piazza, M.R. Bhavani Shankar, and B. Ottersten, "Data predistortion for multicarrier satellite channels based on Direct Learning," IEEE Trans. on Sign. Proc., vol. 62, issue 22, pp. 5868-5880, 2014.

[17]P. Salmi, M. Neri, and G.E. Corazza, "Design and performance of predistortion techniques in Ka-band satellite networks," 22nd AIAA ICSSC, May 2004.

[18]M. Schetzen, "The Volterra and Wiener Theories of Nonlinear Systems," John Wiley Sons, 1980.

[19]M.H. Stone, "The generalized Weierstrass approximation theorem," Mathematics Magazine 21.5, pp. 237-254, 1948.

[20]ESA-funded project "Prototyping and Testing of efficient multicarrier transmission for broadband satellite communications," Ctr. nr 4000112692.